J Mater Sci (2006) 41:6861–6870
DOI 10.1007/s10853-006-0943-5

AFM and SEM characterization of iron oxide coated ceramic membranes

B. S. Karnik · M. J. Baumann · S. J. Masten · S. H. Davies

Received: 4 September 2005 / Accepted: 9 December 2005 / Published online: 1 October 2006

Abstract Alumina–zirconia–titania (AZT) ceramic membranes coated with iron oxide nanoparticles have been shown to improve water quality by significantly reducing the concentration of disinfection by-product precursors, and in the case of membrane filtration combined with ozonation, to reduce ozonation by-products such as aldehydes, ketones and ketoacids. Commercially available ceramic membranes with a nominal molecular weight cut-off of 5 kilodaltons (kD) were coated 20, 30, 40 or 45 times with sol suspension processed Fe_2O_3 nanoparticles having an average diameter of 4–6 nm. These coated membranes were sintered in air at 900 °C for 30 min. The effects of sintering and coating layer thickness on the microstructure of the ceramic membranes were characterized using atomic force microscopy (AFM), scanning electron microscopy (SEM) and energy dispersive x-ray spectroscopy (EDS). AFM images show a decreasing roughness after iron oxide coating with an average surface roughness of ~161 nm for the uncoated and ~130 nm for the coated membranes. SEM showed that as the coating thickness increased, the microstructure of the coating changed from a fine grained (average grain size of ~27 nm) morphology at 20 coating layers to a coarse grained (average grain size of ~66 nm) morphology at 40 coating layers with a corresponding increase in the average pore size from ~57 nm to ~120 nm. Optimum water quality was achieved at 40 layers, which corresponds to a surface coating morphology consisting of a uniform, coarse-grained structure with open, nano-sized interconnected pores.

B. S. Karnik · S. J. Masten · S. H. Davies
Department of Civil & Environmental Engineering,
Michigan State University, East Lansing, MI 48824, USA

M. J. Baumann (✉)
Department of Chemical Engineering & Materials Science,
Michigan State University, East Lansing, MI 48824, USA
e-mail: mbaumann@msu.edu

Introduction

In the United States there is an increasing interest in the application of both ozone and membrane filtration for disinfection by-products (DBPs) and DBP precursor removal in order to meet the requirements of the US Environmental Protection Agency's (US EPA) Surface Water Treatment Rule (SWTR), the Disinfectant and Disinfectant By-products Rule (D/DBPR) and the Long Term 1 Enhanced Surface Water Treatment Rule (LT1ESWTR). During the last decade, researchers have attempted, with limited success, to combine ozonation and polymeric membrane filtration as a water and wastewater treatment option [1–4]. The increasing severity of operating parameters, including higher temperatures and pressures, higher resistance to chemicals and overall durability, made ceramic membranes the natural choice in spite of their much higher costs [5]. Potential applications for ceramic membranes include separation, purification, catalysis and chemical sensors at high temperatures as well as use in chemically reactive environments [6]. Ceramic membranes are ozone resistant and when used in combination with ozone, can achieve stable permeate fluxes without membrane damage [7–11].

Our earlier work showed that stable fluxes could be obtained with ozonation in combination with ceramic membrane filtration [9, 12]. Catalytic degradation of ozone at the membrane surface is thought to oxidize

foulants that accumulate at the membrane surface, thereby preventing membrane fouling. Ozonation–filtration resulted in a reduction of 50% in the dissolved organic carbon (DOC) concentration. It also resulted in the formation of partially oxidized compounds from natural organic matter (NOM) that were less reactive with chlorine, decreasing the concentration of carcinogenic compounds such as trihalomethanes and haloacetic acids. The formation of simulated distribution system total trihalomethanes (SDS TTHMs) and simulated distribution system halo acetic acids (SDS HAAs) were decreased by up to 80% and 65%, respectively [9, 12].

Based on extensive research involving various ozonation methods for drinking water treatment, catalytic ozonation has been determined to be one of the best alternatives for oxidizing NOMs and reducing the demand for chlorine, a common disinfectant used in water purification [13, 14]. In the presence of different metal oxide catalysts, such as iron oxide, manganese oxide, titania, alumina and zirconia, ozone degrades organic compounds, including known harmful and potential carcinogens like saturated carboxylic acids, phenols, aromatic hydrocarbons, dyes, humic substances and herbicides [15]. We have developed a novel procedure based on a layer-by layer method [16] for coating alumina–zirconia–titania (AZT) nano-crystalline ceramic membranes. Iron oxide coated membranes reduced the concentration of DOCs by >85% and the concentrations of SDS TTHMs and SDS HAAs by up to 90% and 85%, respectively, compared to that found with untreated water [15]. Similarly, the iron oxide coated AZT membrane reduced the concentrations of ozonation disinfection by-products (aldehydes, ketones, and ketoacids) in the permeate by >50%, as compared to that obtained using uncoated membranes [15].

Surface modification is significantly affected by surface morphology; it is an important way to enrich the functionality of the ceramic membranes. Atomic force microscopy (AFM), scanning electron microscopy (SEM) and energy dispersive x-ray spectroscopy (EDS) have been used to examine ceramic membrane surfaces. Researchers have successfully characterized the fabrication and microstructure of ceramic membranes derived from alumoxane, ferroxane nanoparticles and Al_2O_3–Al nano-composite powders [17–19]. AFM, SEM and EDS have been used to characterize these coatings on titania membranes, composites of alumina–titania, metal doped ceramics and similar ultra and nanofiltration membranes [19–23].

In this work, AFM, SEM and EDS were used to investigate the surface characteristics of the iron oxide nanolayered coated AZT ceramic membranes. A suspension of iron oxide nanoparticles was passed over the AZT membrane surface 20, 30, 40 or 45 times followed by sintering at 900 °C. The water quality analysis performed on the permeate of different membrane coatings did not show any significant improvement in the reduction of DBPs concentrations neither was there increased removal of DBP precursor with the increase in the number of catalyst coatings [15]. However, the ozonation by-products monitored in the permeate showed a significant reduction in concentration with increasing number of catalyst coatings from 20 to 40. No significant reduction in the concentrations of the ozonation by-products was reported for 60 coatings making 40 coatings the optimum choice in terms of water quality performance and biological stability.

Experimental

Membrane preparation

Tubular AZT (a mixture of alumina, zirconia and titania) ceramic membranes (Clover-leaf design (containing three channels), CéRAM Inside, TAMI North America, St. Laurent, Québec, Canada) with nominal molecular weight cut-offs of 5 kilodaltons (kD) were used as a support for the iron oxide catalytic coatings. The external diameter of each membrane was 10 mm and the active membrane length was 8 cm. The total filtering area of each membrane was approximately 11 cm^2 with each membrane operational from pH 0–14. The initial permeability of the membranes was tested using distilled deionized (DDI) water [8].

A detailed description of the membrane preparation is available in our earlier published work [15]. The colloidal particles used for coating the membranes were prepared using Sorum's method [16]. Transmission electron microscopy (TEM) characterization showed that the average particle diameter was 4–6 nm. The layer-by-layer technique used to coat the membranes is based on a protocol described by McKenzie et al. [16] for coating doped tin oxide electrodes. The membrane was immersed in the colloidal suspension for one minute and then rinsed with DDI water. Then, the membrane was immersed in aqueous phytic acid (40 mM) for one minute and rinsed with DDI water. This sequence was repeated the desired number of times (20, 30, 40 or 45). After coating, the membrane was sintered at 900 °C for 30 min. This temperature was chosen to produce membranes on which the iron oxide particles were

completely sintered to each other and to the membrane surface. These sintered membranes were then examined using AFM, SEM and EDS.

Characterization of membranes

To obtain images of the coated surface of the tubular ceramic membranes, the membrane was first sliced into circular discs of 1 mm thickness using a diamond-wafering saw. Subsequently, these sections were cut to form small arcs of length 3 mm and width 1 mm. These arcs were then mounted on aluminum discs for AFM and aluminum mounting stubs for SEM using carbon adhesive tape. The schematic representation of this procedure is shown in Fig. 1. The samples were then imaged and data collected using AFM, SEM and EDS.

AFM images of the uncoated and coated membranes were obtained using a Nanoscope IV Multimode Atomic Force Microscope (Digital Instruments Inc.), in ambient air in contact mode, which is ideal for examination of textured samples like ceramics. Silicon nitride (Si_3N_4) NP triangular cantilever probes were used to image the iron oxide coated membranes along with uncoated membranes for comparison purposes (Digital Instruments, Veeco Metrology group, CA) with a cantilever spring constant of 0.12 N/m and a frequency of 20 kHz. The tip has a nominal radius of curvature of 20 nm with a height 2.5–3.5 μm and a side angle of 35°. Scans of 20 μm × 20 μm were taken at a scanning rate of ~0.5 Hz. Height and deflection data was taken simultaneously for the same scan area. The 3D surface plot and roughness analysis using the height data were performed on the images to study the surface morphology.

SEM images of the membranes were obtained using a JEOL 6400 V scanning electron microscope equipped with a LaB_6 emitter operated at an accelerating potential of 15 kV at magnifications from 5,000× to 60,000×. The mounted samples were gold coated using an Emscope SC 500 sputter coater at a rate of 7 nm/min with 20 mA current. EDS microanalysis was performed on the samples using a Noran EDS analyzer (Noran Instruments Inc.) at accelerating potential of 20 kV and magnifications ranging from 100× to 5,000×. Samples were carbon coated using an EFFA Mk II carbon coater (Ernest Fullam Inc., Latham NY) in preparation for EDS analysis.

EDS microanalysis has a in built software module to measure the average grain size using the line intercept method. The grain sizes are measured using the average calculated from five micrographs for each sample where on average; 200 grains were measured per micrograph. ANOVA testing was performed on the grain size data within 90% confidence intervals to determine if the differences in the measurements were significant. An identical procedure was followed for the

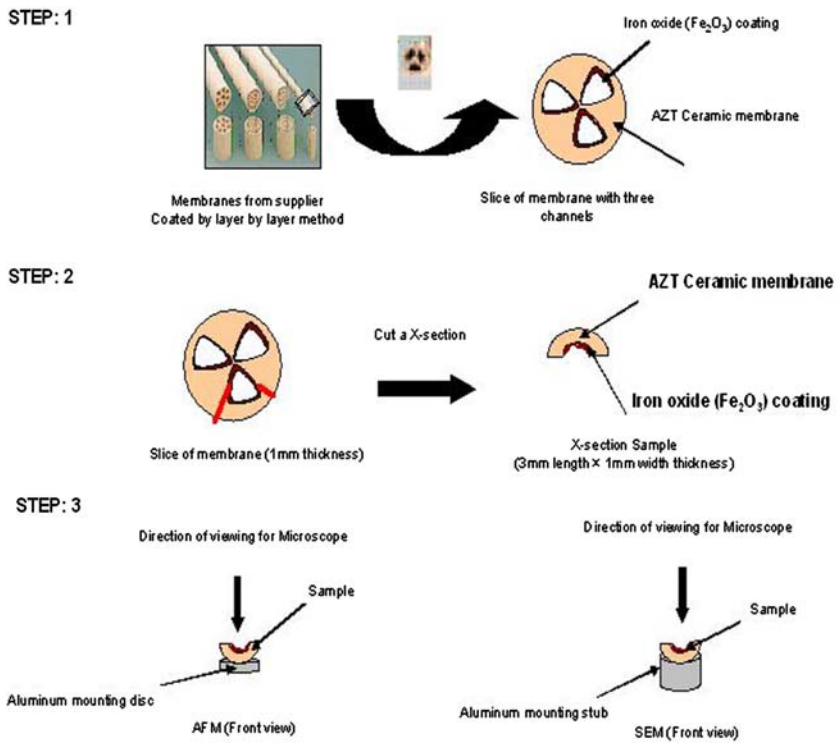

Fig. 1 Schematic representation of sample preparation for SEM and AFM imaging

pore size measurements, however instead of grain size module; arbitrary distance was measured between the grains to determine the pore size.

The natural organic matter (NOM) and the DBP precursors were monitored in terms of dissolved organic carbon concentrations (DOC) [24]. The DBPs total trihalomethanes (TTHMs) and halo acetic acids (HAAs) were measured using standard methods and are reported elsewhere [15–24]. Similarly, ozonation by-products (aldehydes, ketones and ketoacids) were measured using USEPA standard methods [25].

Results and discussion

AFM imaging

AFM analysis provided data on the surface morphology and surface roughness. The manner in which these properties correlate with the surface porosity and filtration performance provide insight into the structure of the filtration membrane. The surface roughness from AFM measurements can be correlated to the grain size found using SEM. Figure 2 a–c shows AFM images of a typical 5 kD uncoated AZT membrane, an uncoated AZT membrane sintered at 900 °C and an AZT membrane coated 40 times with the iron oxide nanoparticle suspension and sintered in air at 900 °C.

For each AFM image, the area in view represents a 20 μm × 20 μm square. The features within any given sample are relatively uniform throughout the sample. With sintering, the surface of the AZT uncoated membrane (Fig. 2a) undergoes a gradual transition from flat featureless regions of ~2.5 μm (±0.2) height to more sharp surface features of ~3 μm (±0.08) height (Fig. 2b). With coating and sintering (Fig. 2c), the height of these features reduces to ~1.5 μm (±0.1). When comparing membranes coated for 20, 30 and 40 times followed by sintering, the respective AFM height data (plotted in Fig. 3) show no statistical difference between membranes coated 30 and 40 times. However, both are significantly decreased in comparison to the membranes coated 20 times.

However, while the height of each feature is not significantly reduced as the number of coats increases (Fig. 4), there is an increase in the number of these features. This result is substantiated by AFM roughness analysis which shows a significant decrease in roughness from ~161 nm to ~78 nm upon sintering of the uncoated AZT membrane. There is also a reduction in the surface roughness from ~161 nm for the uncoated membrane to an average of ~130 nm for the coated membranes, with no statistical difference in the roughness with an increase in the number of coats.

For all membranes tested, the observed magnitude of the roughness, shown in Fig. 5, is much greater than the size of the original iron oxide particles (4–6 nm). As shown in the SEM micrographs in Fig. 6, this increase in roughness is due to interparticle sintering between the iron oxide nanoparticles and, given the integrity of the iron oxide nanocoating, a result of the coating sintering to the underlying porous ceramic AZT membrane.

SEM imaging

The SEM micrographs (Fig. 6) of the coated AZT ceramic membranes exhibit a similar coarsening behavior of the membrane surface with increases in the size and number of surface grains with number of coats, as was found using AFM (Fig. 4a–c). The nanoparticles on the surfaces have sintered together and there is an overall coarsening of the surface (increase in the average grain size) as the number of coatings increases from 20 to 40.

The average grain size for the membrane surfaces are plotted in Fig. 7. After sintering for 30 minutes, the average grain size increased from ~21 nm (±0.24), for the uncoated membranes, to ~66 nm (±20.0) for the coated membranes. Further increasing the number of coatings from 20 to 30 and subsequently 30 to 40, resulted in a significant increase in the average grain size from ~27 nm (±10) to ~31 nm (±11) to ~66 nm (±23) respectively. This particle growth is likely a result of the large driving force for sintering posed by the high surface area of these nanosized particles, whereby agglomerated regions of nanoparticles rapidly sinter and are separated by larger pores [26]. This finding is verified by noting that both the average *grain* size for the sintered membranes coated 40 times (Fig. 7, 5 kD-40–900 °C) and the average *pore* size following sintering (Fig. 8, 5 kD–40–900 °C) have both increased over those average grain and pore sizes reported for 20 and 30 coatings. This indicates that a greater degree of agglomeration of the iron oxide particles has occurred for membranes coated 40 times.

With 45 coatings, no significant increase in porosity is observed, and more importantly, no water quality improvements were found [27], making 40 coatings a critical processing parameter. So, while the average surface pore size has increased from 40 nm (±10) for the uncoated membrane to 120 nm (±40) for the membranes coated 40 times, the more open porosity has significantly increased the water quality while maintaining the average pore size at the nanoscale.

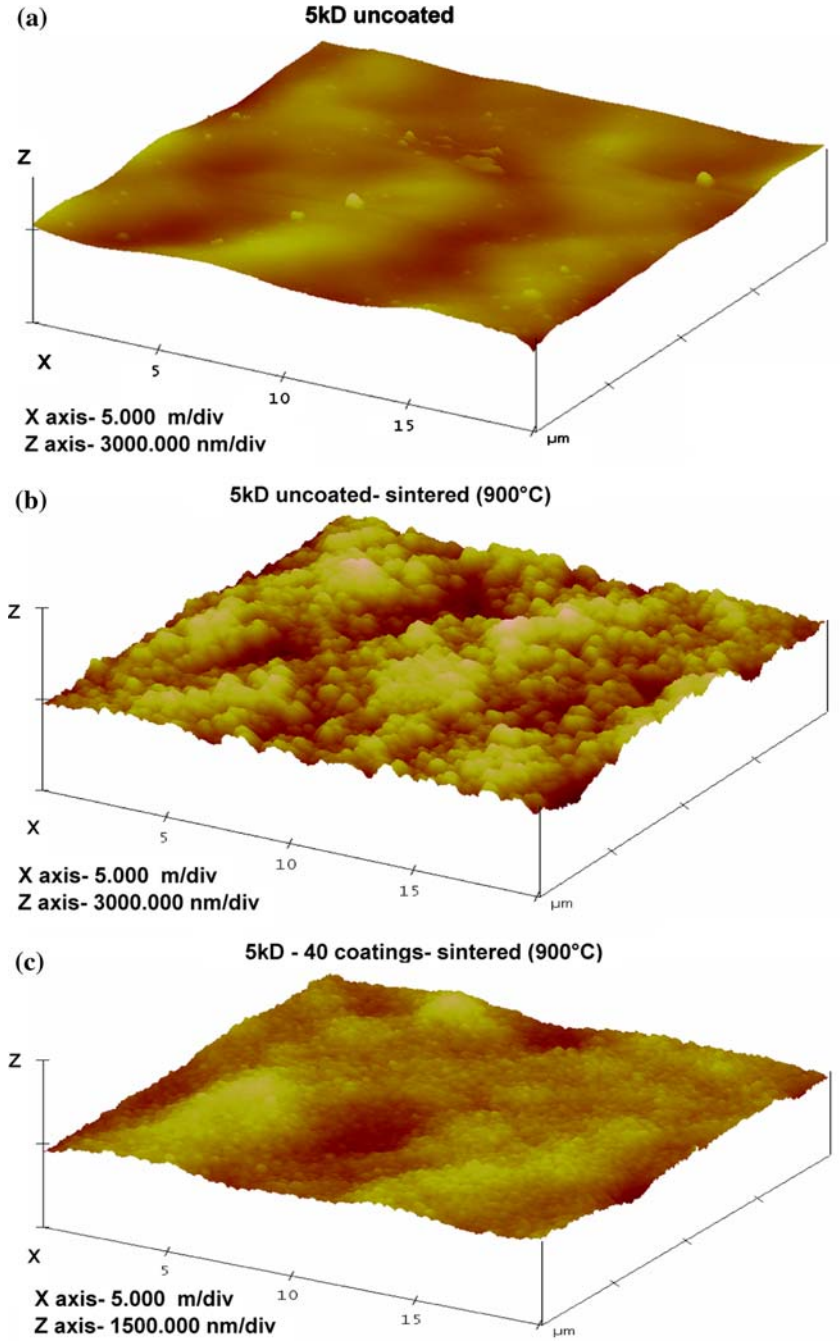

Fig. 2 AFM images of the AZT ceramic membranes: (**a**) 5kD MWCO AZT membrane uncoated, (**b**) 5 kD AZT membrane uncoated, sintered at 900 °C for 30 min and (**c**) 5 kD AZT membrane with 40 coatings of iron oxide, sintered at 900 °C for 30 min

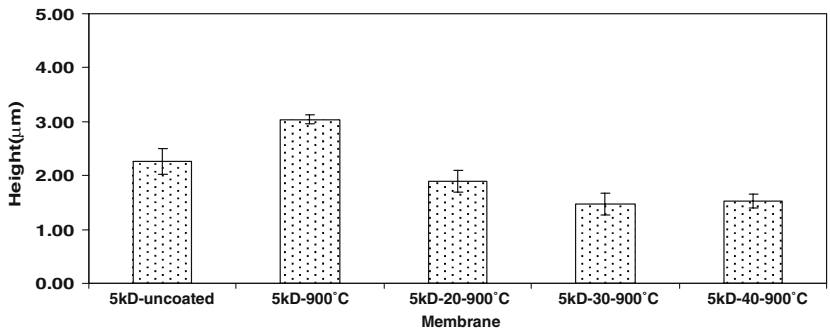

Fig. 3 Height data for AFM images of membranes with different number of coatings

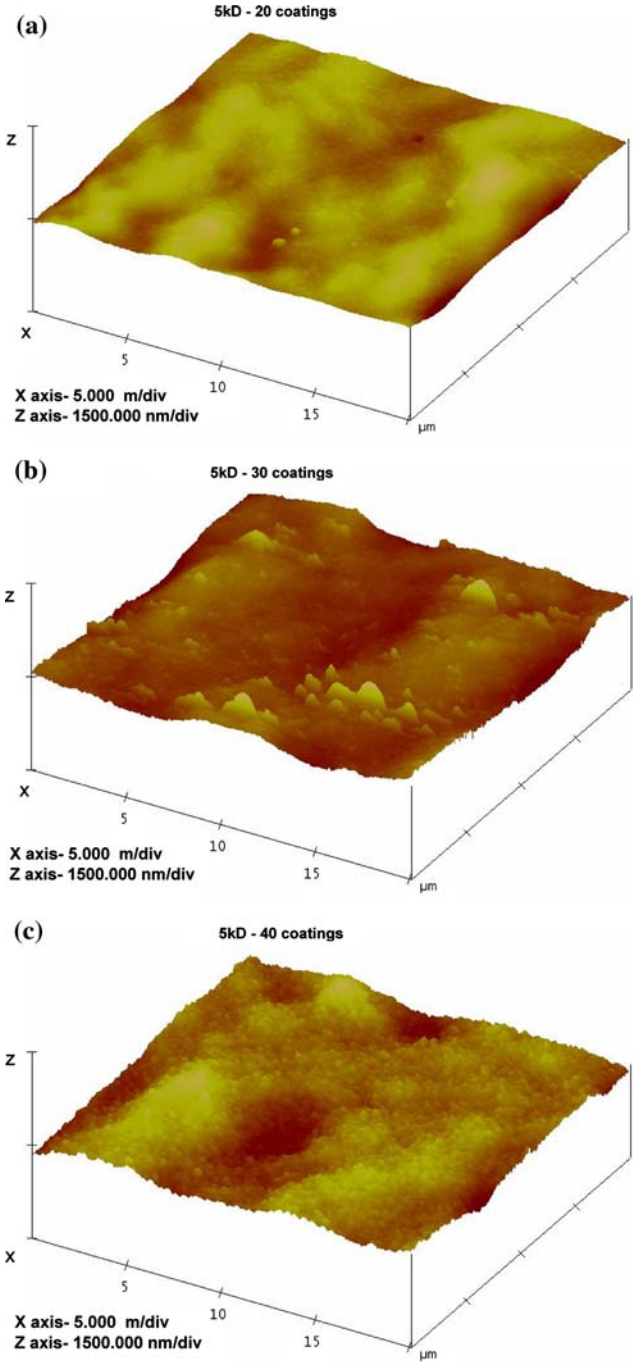

Fig. 4 AFM image of an AZT ceramic membrane with iron oxide coating: (**a**) 5 kD AZT membrane with 20 coatings of iron oxide, sintered at 900 °C for 30 min, (**b**) 5 kD AZT membrane with 30 coatings of iron oxide, sintered at 900 °C for 30 min and (**c**) 5 kD AZT membrane with 40 coatings of iron oxide, sintered at 900 °C for 30 min

SEM micrographs (Fig. 6) show a clear evidence of uniform coverage of coating and sintering as verified by AFM results shown in Figs. 2 and 4. Also the coarsening of the membrane surface explains the decrease in roughness value from uncoated membranes to coated and sintered membranes.

Energy dispersive x-ray microanalysis (EDS) mapping was done for Ti, Al, Zr, O and Fe. EDS mapping of the uncoated AZT membrane (Fig. 9a) showed a uniform distribution of titania and zirconia over a porous alumina matrix. The skin of the as-received uncoated membrane was therefore a mixture of titania and zirconia which formed an ultrafiltration layer (ultrafiltration occurs between microfiltration (10^{-6} m) and nanofiltration (10^{-9} m)). EDS mapping of a coated and sintered membrane (Fig. 9b) confirmed the morphology and composition of the uncoated membrane with the addition of an iron oxide layer predominantly present at the surface, with a uniformly diffused iron oxide presence into the membrane surface. This uniform distribution of iron oxide into the membrane could be a result of capillary action during the coating process and/or a result of the diffusion of iron oxide nanoparticles in the sintering process.

As expected, EDS line scans for the membranes coated 20, 30 and 40 times revealed a corresponding increase in the concentration of iron (Fe) present in the membrane surface. The Fe concentration was proportional from 20 to 30 to 40 coatings (Fig. 10).

The water quality data shown in Fig. 11 gives evidence as to how the catalyst coating has improved water quality performance in terms of reducing DBP precursors when compared to uncoated membranes. Iron oxide coated ceramic membranes were superior in terms of performance as compared to uncoated ceramic membranes in terms of DBP precursors as well as DBPs as shown in Fig. 11. DOC concentrations showed a significant decrease for the Fe_2O_3 catalyst coated ceramic membranes with increasing Fe_2O_3 coating layers when compared to uncoated membranes. Our earlier work details the improvement in water quality for Fe_2O_3 catalyst coated ceramic membranes with different treatment processes in comparison to the uncoated ceramic membranes [15]. Fe_2O_3 catalyst coated ceramic membranes are a promising tool for reducing the ozonation by-products which serve as substrates for growth of microorganisms. This reduces their regrowth potential in the permeate making the water more biologically stable and safe for consumption. Further, the figure shows no significant changes in the water quality in terms of measured concentration of DBPs like TTHMs and HAAs with increasing Fe_2O_3 catalyst coating layers from 20 to 40 coats. A concomitant decrease in the ozonation by-products was seen with increasing number of Fe_2O_3 coating layers, however, no significant changes in the concentrations were reported beyond 40 coating layers.

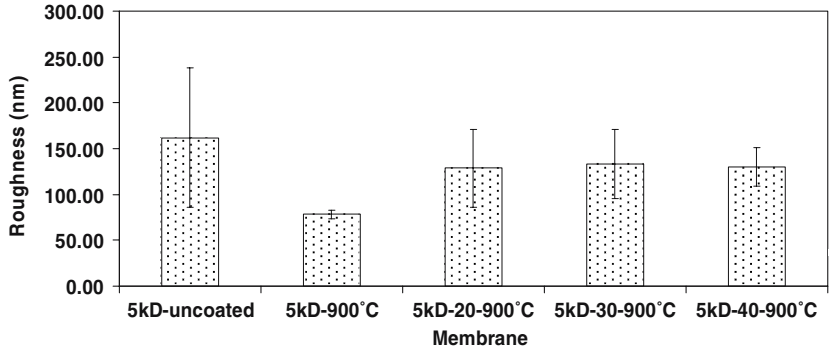

Fig. 5 Roughness data for AFM images of membranes with different number of coatings

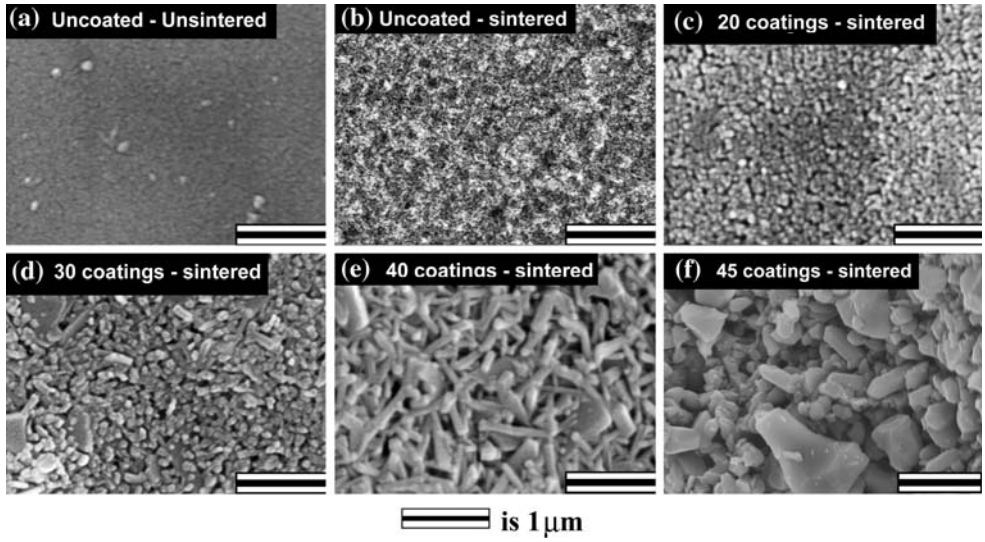

Fig. 6 SEM images of an AZT ceramic membrane: (**a**) 5 kD MWCO AZT membrane uncoated, (**b**) 5 kD AZT membrane uncoated, sintered at 900 °C for 30 min and (**c–f**) 5 kD AZT membrane with 20, 30, 40, 45 coatings, respectively, of iron-oxide, sintered at 900 °C for 30 min

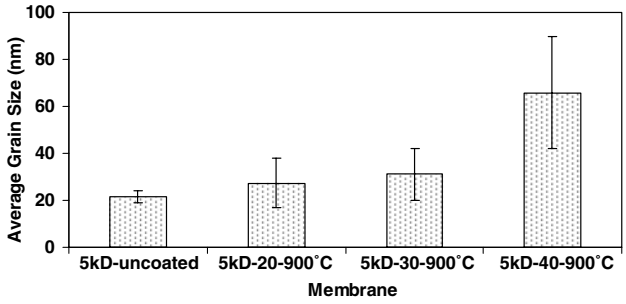

Fig. 7 Grain size measurements of AZT ceramic membrane: Membranes: 5 kD MWCO uncoated, 5 kD with 20, 30, 40 coatings of iron oxide sintered at 900 °C for 30 min

AFM characterization showed a decrease in the surface roughness of the ceramic membrane with Fe2O3 coating which led to an improved effective filter separation layer most likely comprised of nano-sized iron oxide grains. SEM micrographs show a nanoscale average pore size and uniform coverage of the coating layers, not only across the ceramic membrane surface, but also into the membrane itself. This has likely led to the catalytic reactions that resulted in a significant improvement of water quality in terms of removal of disinfection by-products and ozonation by-products shown in Fig. 11. The increased Fe concentration into and away from the outer membrane surface, as measured by EDS, further supports the explanation given for the improved water quality data for the ceramic membranes coated with 40 layers of Fe_2O_3 nanoparticles.

Conclusions

Coating and sintering of AZT membranes with nanoscale iron oxide particles resulted in significant changes in the membrane surface morphology as a result of sintering and coarsening of the coating nanoparticles. SEM details the changes in surface morphology of the coated membrane where the surface morphology changes from a fine grained uniform structure at 20 coats to a coarser grain uniform structure at 40 coats. SEM also captured the change in the average pore size,

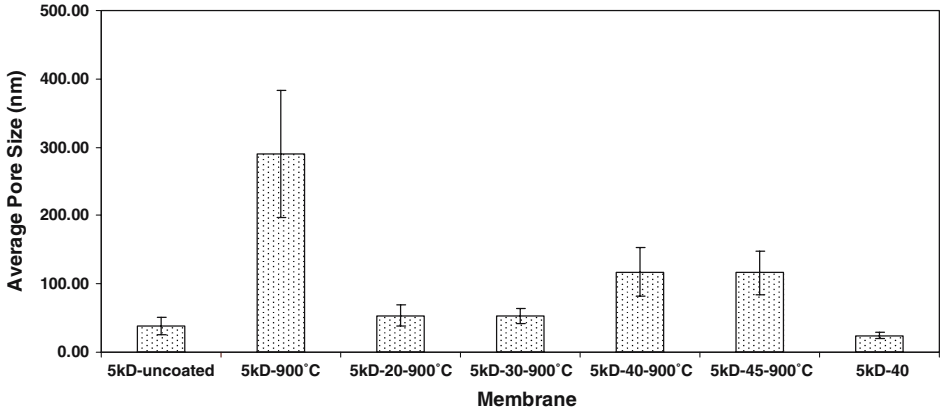

Fig. 8 Average pore size measurements for the AZT membranes: 5 kD MWCO uncoated, 5 kD sintered at 900 °C for 30 min, 5 kD with 20, 30, 40, 45 coatings of iron oxide sintered at 900 °C for 30 min and 5 kD with 40 coatings of iron oxide unsintered

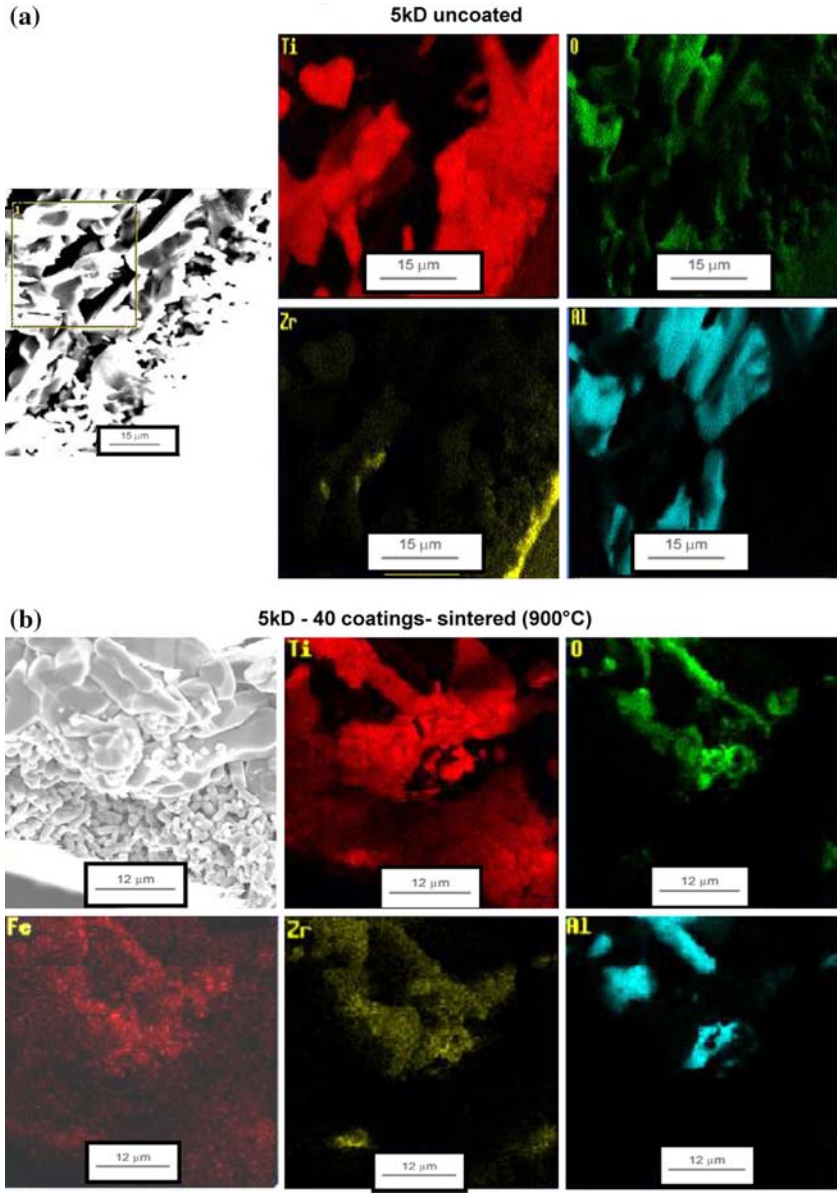

Fig. 9 EDS mapping of the membranes: EDS mapping of uncoated membrane and (**b**) EDS mapping of membrane with 40 coatings and sintered at 900 °C for 30 min

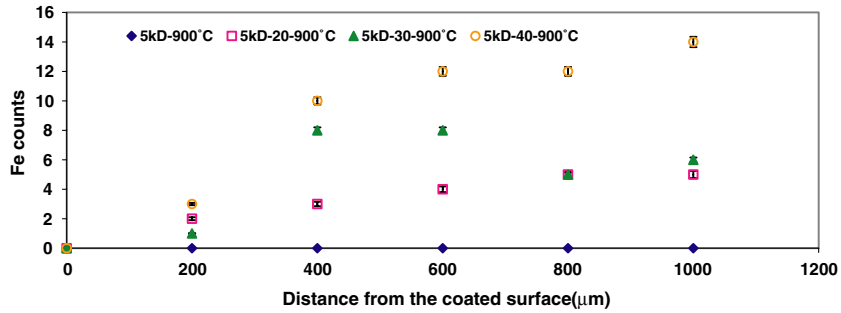

Fig. 10 Relative Fe concentration from EDS scans. The graph represents relative Fe concentrations measured as Fe counts in the EDS scans

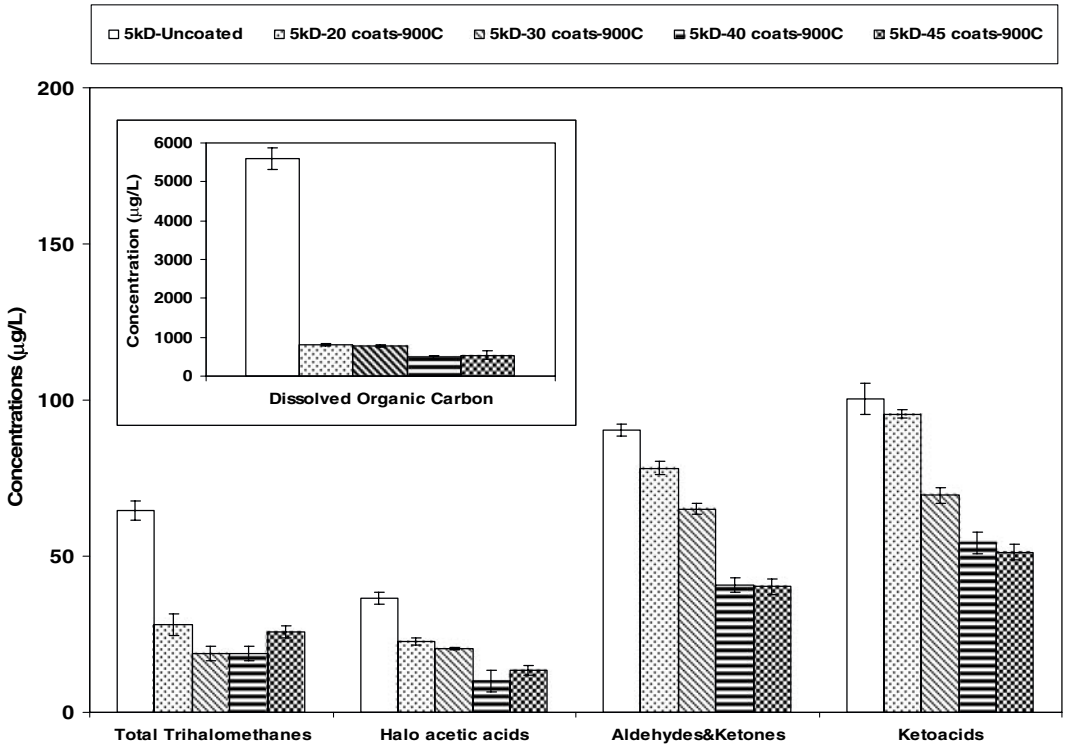

Fig. 11 Water Quality data for the permeate after combined ozonation membrane treatment process. The data for water quality parameters for a 5 kD AZT membrane uncoated, unsintered, with 20, 30, 40, 45 coatings of iron-oxide, sintered at 900 °C for 30 min. The insert in the graph is the plot of dissolved organic carbon concentrations for the same membranes. Experiment details [15]

from the micropores in the underlying AZT membrane to the nanopores within the iron oxide surface layer of the coated membrane. This decrease in porosity into the nanopores regime is one possible reason for the improved performance of these iron oxide coated ceramic membranes over uncoated membranes. AFM and SEM data are consistent, where decreasing surface roughness correlates with a coarsened average grain size on both the sintered uncoated and coated membranes, with the smoothest and coarsest surface existing at 40 coats, which is the optimum in terms of water filtration [15]. It is at 40 layers that we have the largest average pore size (although still in the nanopores range at 120 nm (±40)) and largest average grain size that results from the greater degree of agglomeration of the iron oxide particles during the coating process. Capillary action during the coating process, and/or diffusion during sintering, results in the uniform distribution of iron oxide particles throughout the membrane interior. This further enhances water filtration because of the increased exposure to the catalytic iron oxide, not only at the membrane surface, but into the membrane itself. Ongoing studies using SEM of coated and unsintered membranes will determine whether capillary forces during the coating application process are sufficient to drive the iron oxide nanoparticles into the interior of the membrane. We have found that 40 coats of the nanosized iron oxide particles on the underlying AZT

ceramic membrane is the optimum coating in terms of water quality performance which meets the stringent EPA regulatory requirements, while still in the regime of nanofiltration. Future research will examine the mechanisms for the degradation of NOM and the removal of harmful DBPs by the iron oxide coated AZT ceramic membranes.

Acknowledgments The authors would like to acknowledge the US Environmental Protection Agency (US EPA) Science To Achieve Results (STAR) Program (Grant No. RD830090801) for financial support of this work. Our thanks also go to Ms. Ewa Danielewicz, from the Center for Advanced Microscopy for her assistance during SEM sample preparation. Dr. Hazel Hosein from the Composite Materials and Structures Center is also acknowledged for her assistance during the AFM work. We would also like to thank Mr. David Jackson for his assistance with the membrane coating process.

References

1. Shanbhag P, Guha A, Sirkar K (1998) Ind Eng Chem Res 37:4388
2. Castro K, Zander A (1995) J Am Wat Works Assoc 87:50
3. Shen Z, Semmens M, Collins A (1990) Environ Technol 11:597
4. Hashino M, Mori Y, Fujii Y, Motoyama N, Kadokawa N, Hoshikawa H, Nishijima W, Okada M (2000) Water Sci Technol 41:17
5. Zuzek E, Catán S, Arciprete C, Dimitrijewits M, Almandoz M, Marchese J (2001) Granul Matter 3:145
6. Zeng Z, Xiao X, Gui Z, Li L (1997) J Membr Sci 136:153
7. Kim J, Somiya I (2001) Environ Technol 22:7
8. Kim J, Somiya I, Fujii S (1999) In: Proceedings of the 14th Ozone World Congress, Dearborn, August 1999, p.131
9. Karnik B, Davies S, Chen K, Jaglowski D, Baumann M, Masten S (2005) Water Res 39:728
10. Schlichter B, Mavrov V, Chmiel H (2004) Desalination 168:307
11. Allemane H, Deloune B, Paillard H, Legube B (1993) Ozone Sci Eng 15:419
12. Karnik B, Davies S, Baumann M, Masten S (2005) Water Res 39:2839
13. Allemane H, Deloune B, Paillard H, Legube B (1993) Ozone Sci Eng 15:419
14. Volk C, Roche P, Joret J, Paillard H (1997) Water Res 31:650
15. Karnik B, Davies S, Baumann M, Masten S (2005) Environ Sci Technol 39:7656
16. Mckenzie K, Marken F, Hyde M, Compton R (2002) New J Chem 26:625
17. Cortalezzi M, Rose J, Barron A, Weisner M (2002) J Membr Sci 205:33
18. Cortalezzi M, Rose J, Wells G, Bottero J, Barron A, Weisner M (2003) J Membr Sci 227:207
19. Lu H, Hu J, Chen C, Sun H, Hu X, Yang D (2005) Ceram Int 31:481
20. Chou K, Kao K, Huang C, Chen C (1999) J Porous Mater 6:217
21. Bae D, Cheong D, Han K, Choi S (1998) Ceram Int 24:25
22. Pedersen H, Tranto J, Høj J (1997) Key Eng Mater 132–136:1707
23. Siriwardane R, Poston J Jr, Fisher E, Lee T, Dorris S, Balachandran U (2000) Appl Surf Sci 167:34
24. Clesceri L, Greenberg A, Eaton A (eds) (1998) Standard methods for examination of water & wastewater. American Public Health Association Publishing
25. Munch J, Munch D, Winslow S, Wendelken S, Pepich B (1998) Method 556: Determination of carbonyl compounds in drinking water by pentafluorobenzylhydroxylamine derivatization and capillary gas chromatography with electron capture detection. USEPA, Cincinnati, OH
26. Barsoum M (2003) Fundamentals of ceramics. Institute of Physics Publishing, pp. 336
27. Karnik B (2006) The use of ozonation and catalytic ozonation combined with nanofiltration for the control of natural organic matter (NOM) and disinfection by-products (DBPs) in drinking water. Michigan State University, to be submitted May 2006